# City, University of London Institutional Repository

This is the accepted version of the paper.

This version of the publication may differ from the final published version.

# Loss of Müller cells and photoreceptors in Macular Telangiectasia Type 2

Michael B Powner, PhD,[1] Mark C Gillies, MBBS, PhD,[2] Meidong Zhu, MBBS, PhD,[2,3] Kristis Vevis, MSc (Hons),[1] Alex P Hunyor, MBBS, FRANZCO,[2,4] and Marcus Fruttiger, PhD[1]

1) UCL Institute of Ophthalmology, University College London, London, UK
2) Save Sight Institute, University of Sydney, Australia
3) Lions New South Wales Eye Bank, Sydney and Sydney Eye Hospital, Australia
4) Retinal Therapeutics Research Unit, University of Sydney, Australia

**Running title**: Müller cell and photoreceptor loss in MacTel type 2

**Corresponding author contact information:** m.fruttiger@ucl.ac.uk

**The following material should appear online only:** Figure 3 and 4

**Abstract**

PURPOSE: To correlate postmortem histology from a MacTel type 2 patient with previously recorded clinical imaging data.

DESIGN: Observational clinicopathological case report

METHODS: The distribution of retinal blood vessels was used to map the location of serial wax sections in color fundus and optical coherence tomography (OCT) images. Fluorescent immunohistochemistry was used to visualize markers for Müller cells (vimentin and RLBP1), photoreceptors (LM-opsin, rhodopsin and COX2) and the outer limiting membrane (ZO-1 and occludin).

MAIN OUTCOME MEASURES: Distribution of specific markers in immunohistochemistry on retinal sections through the fovea in relation to clinical data.

RESULTS: The clinically recorded region of macular pigment loss in the macula correlated well with Müller cell depletion.  OCT data showed a loss of the photoreceptor inner segment/outer segment junction (IS/OS) in the central retina, which correlated well with rod loss but not with cone loss.  Markers for the outer limiting membrane were lost where Müller cells were lost.

CONCLUSIONS: We have confirmed our previous finding of Müller cell loss in MacTel type 2 and have shown that the area of Müller cell loss matches the area of macular pigment depletion. In this patient the IS/OS junction seen by OCT was absent in a region where rods were depleted but cones were still present.

## INTRODUCTION

Macular telangiectasia (MacTel) type 2, also known as idiopathic juxtafoveolar telangiectasia type 2, is usually bilateral and can lead to legal blindness. The name of the disease is based on characteristic fluorescein angiographic changes in the macula, originally described by Gass.[1]  However, there are several additional disease signs, including loss of macular transparency, superficial white crystals, depletion of macular pigment and progressive foveal thinning.[2-6] Furthermore, optical coherence tomography has identified hyporeflective spaces in the inner and outer retina in some patients.[5-8]  More advanced cases may also develop clumps of pigment cells in the retina and less commonly, subretinal neovascularisation.[2] Visual symptoms are usually first noticed in the fifth to sixth decade and include reading difficulties and loss of visual acuity.[9;10]  During the early stages of MacTel type 2 central scotopic function is reduced; more advanced cases usually develop dense scotopic and photopic scotomas in the perifovea.[11-13]  The cause of the disease is not known, and no treatment is known to prevent the progressive loss of central vision.

We have previously reported a clinicopathologic analysis of a postmortem eye from a MacTel type 2 patient, finding a loss of Müller cells in the macula.[14]  We hypothesized that this specific loss of Müller cells may be a critical component of MacTel type 2 pathology but so far the anatomical basis of the specific losses in visual function is not clear.  We have now obtained postmortem eye samples from a second MacTel type 2 patient and correlated histopathological changes in photoreceptors with clinical data from this patient, including spectral domain optical coherence tomography (OCT), providing an anatomical rationale for the functional deficits in this particular patient.

## MATERIALS & METHODS

*Donor*

The donor was female and diagnosed with MacTel type 2 in 1992 at the age of 52. A glucose tolerance test (2007) showed a fasting plasma glucose of 6.5 mmol/L and a 2h plasma glucose of 10.4 mmol/L indicating impaired glucose tolerance but not diabetes mellitus. Blood glucose levels were monitored since then and her fasting plasma glucose level was never over 8 mmol/L and HbA1C was below 7% (under diet control only). This may be a possible explanation of why she did not develop diabetic retinopathy. In 2007 the patient was diagnosed with scleroderma. According to her ophthalmologist she had retinal arteriolar abnormalities (premature arterial disease).

*Tissue processing*

Institutional review board (IRB)/ethic committee approval was obtained. The time elapsed between death and fixation of the eyes in this study was 3.5 hours. The left eye was fixed in 4% paraformaldehyde (PFA) for 64 hours and then kept in 1% PFA for 3 weeks. Subsequently the anterior parts of the eye were removed and the eye was flattened (using four radial incisions) and photographed. A region that included the optic disc and fovea was dissected from the eye and processed for wax embedding. Because in our previously studied sample[14] the retina split horizontally during embedding we used here a soft sponge to stabilize the tissue and apply gentle pressure during wax processing. Once embedded, naso-temporal sections were cut at 6 μm and mounted onto Superfrost® plus slides (VWR). Sections were deparaffinized with xylene and rehydrated through graded alcohols and processed for immunohistochemistry.

*Immunohistochemistry*

Antigen retrieval was carried out by heating the slides to 125ºC in 90% glycerol (molecular grade) and 10% 0.01M citrate buffer pH6.0 for 20 minutes in a pressure cooker. Sections were then briefly washed in water, incubated for 1 hour at room temperature in blocking buffer (1% BSA, 0.5% triton X-100 in PBS) and then in primary antibody (diluted 1:200 in blocking buffer) either at room temperature for 1 hour or overnight at 4°C. Primary antibodies used were: vimentin-Cy3 (Sigma, C9080), RLBP1 (AffinityBioReagents, MA1-813), GS (Chemicon, MAB302), rhodopsin (Chemicon, MAB5356), ML-opsin (Millipore, AB5405), ZO-1 (Invitrogen) and occludin (Invitrogen). Sections were washed in washing buffer (0.1% tween20 in

4

PBS) and incubated for 1 hour at room temperature in secondary antibodies (Invitrogen, diluted 1:200 in blocking buffer).  Subsequently sections were washed in washing buffer, treated with Hoechst (10µg/ml in washing buffer) for 30 seconds, washed again and mounted in Moviol mounting medium (Sigma).  Images were taken using a Leica DM IRB fluorescent microscope and/or a Zeiss LSM700 confocal microscope.

**RESULTS**

*Clinical features*

The 61 year old female donor died in May 2011 from respiratory failure.  The patient suffered from scleroderma and end stage interstitial pulmonary fibrosis.  She was diagnosed with MacTel type 2 by one of the authors (APH) in 1992.  Later she was also diagnosed with type 2 diabetes (impaired glucose tolerance in 2007 and diabetes mellitus in 2009).  The diabetes was controlled with diet only and diabetic retinopathy was never diagnosed at any stage.  Increased prevalence of diabetes, but minimal diabetic retinopathy in MacTel type 2 patients has previously been reported.[15-18]  A fluorescein angiogram taken in March 2009 showed typical features of MacTel type 2 with telangiectatic vessels particularly in the temporal macula and diffuse staining in later images of both eyes (Fig. 1A, B). At the same visit optical coherence tomography (OCT) on the left eye showed hyporeflective spaces in the fovea (Fig.  1C) and discontinuity of the main hyper-reflective line in the photoreceptor layer (a line that is usually referred to as the inner/outer segment junction or IS/OS).  This line was missing in the fovea and the temporal macula (arrowheads in Fig. 1 C).  Photopic microperimetry (MP) showed a scotoma in the temporal macula (Fig. 1 D).  Similar findings were made in the right eye (not shown). One year later, in 2010 (one year before death) the donor's last ophthalmic examination showed an almost symmetric loss of the IS/OS in the temporal and nasal macula of each eye (arrows in Fig. 1E).  However, the location of the scotoma was still predominantly temporal (Fig. 1F).  At that stage her visual acuity was OD 20/125 and OS 20/125. Fundus color photographs showed localized clumping of pigmented cells in the temporal perifovea (Fig. 1G). Fundus autofluorescence showed hyper-autofluorescence due to a lack of masking of background normally caused by high levels of macular pigment in the central macula (Fig. 1H).

*Macular pigment*

Macroscopic examination of the fixed postmortem eye revealed loss of macular pigment in an oval area in the central retina (Fig. 2A), similar to our findings in the previously published postmortem case.[14]  This is hallmark feature of MacTel type 2 confirms the diagnosis.[3;4;19]  Unfortunately, clinical data showing specifically the distribution of macular pigment, such as dual wavelength autofluorescence,[4;19] was not available.  However, the color fundus image (Fig. 1G) contained sufficient color information to spatially localize the distribution of macular pigment loss.  To this end we isolated the blue channel in the color fundus image and enhanced the contrast

(Fig. 2B). This revealed a bright central oval area that matched the shape and location of macular pigment distribution in the macroscopic image (Fig. 2A). The oval area also correlated well with clinical data obtained in other patients by confocal blue light imaging or dual wavelength macular pigment measurements.[3;4;19] We therefore used the information in the blue channel from the fundus color image to plot the distribution of macular pigment in the color image (dotted circle in Fig. 2C).

### Matching of clinical data with histology

In order to correlate postmortem histology with clinical data that was recorded before the donor's death, we used the distribution of blood vessels to spatially match serial wax sections onto the color fundus image as previously described.[14] This is illustrated in figure 2C where the nasal to temporal location of vessels (white dots in Fig. 2C) in 3 different sections (350, 405 and 485) correlated well with the color fundus image. Based on this, we then used immunohistochemistry to correlate the distribution of specific cell populations with clinical imaging modalities.

### Müller cell loss

In the first instance we visualized Müller cells with an antibody against vimentin on a section (404) through the fovea (Fig. 2D). We have previously shown that in postmortem retina from healthy donors vimentin is expressed throughout the retina.[14] However, in the MacTel type 2 retina we found a dramatic loss of Müller cells in the central retina that matched the area of macular pigment loss (Fig. 2C, D), confirming our findings in the previous MacTel type 2 case study.[14] This was illustrated by plotting the lateral distribution of Müller cells (horizontal red bars in Fig. 2D), which showed close correlation with macular pigment distribution (yellow arrows in Fig. 2D). Higher magnification of the vimentin immunohistochemistry also showed a good correlation between macular pigment loss (yellow arrows in Fig. 2C-F) and a loss of Müller cell processes in the inner and outer nuclear layers. In the temporal macula the location of a large vessel (stars in Fig. 2C, F) confirmed the accuracy of the matching between the fundus image and the histology in this section. Additional sections from the superior and inferior macula showed smaller regions of Müller cell depletion that also matched well with the area of macular pigment loss (not shown). Labeling with an alternative marker for Müller cells, glutamine synthetase (GS, not shown) and retinaldehyde binding protein 1 (RLBP1, also known as CRALBP, Fig. 4G) showed the same loss of staining in the central retina. This was also the case in our previous MacTel 2 case, further suggesting a loss of cells rather than a downregulation of a specific marker. Moreover, in our previous case the wax

embedding procedure caused horizontal splitting of the retina. Here we observed the same horizontal splitting again (Fig. 2D-F), despite our efforts in this case to avoid this processing artifact by using a sponge to gently depress the tissue during wax embedding. Glial fibrillary acidic protein (GFAP) was only detected in retinal astrocytes (not shown), demonstrating the absence of reactive Müller cells, as in the previous case.[14]

A lack of functional Müller cells may impact on inner retinal neurons. In the previous case we have shown the presence of nuclei in the inner nuclear layer but at slightly reduced numbers. Here, hematoxylin-eosin (H&E) staining also revealed the presence of numerous nuclei in the inner nuclear layer (Fig. 3, available at http://aaojournal.org) indicating that the majority of these neurons survive. To further probe the state of inner retinal neurons we used an antibody against protein kinase C alpha (PRKCA, also known as PKC alpha), which is a marker for rod bipolar cells.[20] Similar to rods these cells become more sparse towards the fovea in normal retina.[21] In a central section (404) we found strong expression in the periphery and reduced staining towards the fovea (Fig. 4A-C, D, G, available at http://aaojournal.org). However, PRKCA positive cells could be found centrally to the boundaries of Müller cell and rod loss (Fig. 4 E, F, available at http://aaojournal.org), suggesting rod bipolar cells are not directly affected by either Müller cell or rod depletion.

### *Cone photoreceptors*

Previous studies using OCT on MacTel type 2 patients have shown breaks in the IS/OS and linked those abnormalities to functional deficits.[7;22] We therefore attempted to correlate the OCT data from our MacTel type 2 donor with tissue histology. To this end we used the vessel shadows in the projection map of the OCT B-scans to match the color fundus image (Fig. 5A). Furthermore, we traced breaks in the IS/OS line in each B-scan and mapped this onto the projection map (blue area in Fig. 5A). The OCT scanning axis (green line in Fig. 5A) was not exactly in register with the direction of our histological sectioning (white line in Fig. 5A). Nevertheless, the lateral distribution of the IS/OS break was similar in the central OCT B-scan axis (green line and black arrows in Fig. 5A, B) compared to the location of section 409 (white line and blue arrows in Fig. 5A, C).

In the first instance we aimed to correlate the IS/OS break (blue arrows in Fig. 5) with immunohistochemical staining of cone photoreceptors (in section 407). An antibody against LM-opsin revealed strong staining of outer segments and weaker staining of

the entire photoreceptors (red in Fig. 5C-F). Previous studies have linked the IS/OS signal with the ellipsoid region, [23-25] the mitochondria rich distal portion of the cone inner segment.[26] We therefore used an antibody against cytochrome oxidase 2 (COX2) to label mitochondria (green in Fig. 5C-F). In the photoreceptor layer the COX2 stain revealed small oval structures adjacent to cone outer segments, presumably ellipsoids (Fig. 5D-F). The lateral distribution of the COX2 positive ellipsoids and LM-opsin positive outer cone segments correlated well (horizontal green and red bars in Fig. 5C). Surprisingly, this did not match with the IS/OS in the OCT scan (blue arrows in Fig. 5). Particularly in the nasal macula the IS/OS was absent, whereas the immunohistochemistry showed largely intact cone photoreceptors in this area. Nevertheless, two small patches of complete photoreceptor loss in the fovea (stars in Fig. 5F) corresponded well with the hyporeflective cavities seen in the OCT in the fovea (Fig. 5B). H&E staining of a neighboring section (403) shows no structures inside those cavities (or cysts) suggesting that they are fluid filled in vivo. Furthermore, a large area of cone depletion was observed in the temporal parafovea (arrowheads in Fig. 5E, F), which might explain the large, predominantly temporal scotoma recorded in the patient before death (Fig. 1D, F).

### Rod photoreceptors

To further investigate cellular correlates to the IS/OS loss (Fig. 5A, B) we visualized rod photoreceptors with an antibody against rhodopsin (green in Fig. 5G-I) and their lateral distribution was plotted (green horizontal bars in Fig. 5G) in section 409. This revealed a large rod free area in the central macula that corresponded well with the IS/OS loss seen in the OCT (blue arrows in Fig. 5G). Higher magnification of the region where the rod stain is discontinued further demonstrated the close correlation with the IS/OS break (Fig. 5H, I). As in the previous section (Fig. 5C-F) cones were stained for LM-opsin (red) and were only depleted in the temporal macula.

### Outer limiting membrane

Since we found large areas of Müller cell and rod photoreceptor loss, we investigated the structure where these two cell types interact, the outer limiting membrane (OLM). The OLM is a planar array of adherens junctions between Müller cell processes and photoreceptors, which may influence the orientation and light guiding properties of photoreceptor outer segments and thereby possibly signals in OCT. The OLM can be detected by OCT as a fine line internal to the IS/OS.[23] In our patient this line

could be detected (Fig. 1E, 5B) up to the region where the IS/OS line was disrupted, but could not be identified further centrally.

For immunohistochemistry we used an antibody against the tight junction protein 1, also known as zona occludens 1 (ZO-1), to visualize the OLM (red in Fig. 6A-F) and to relate its distribution to the OCT data and to Müller cells and rod distribution (in section 410). In the peripheral retina ZO-1 was found in the OLM (white arrowheads in Fig. 6B, E). Furthermore, we found staining in the outer plexiform layer (stars in Fig. 6B, C) and in blood vessels (e.g. next to yellow arrow in Fig. 6C). The ZO-1 labeling of the OLM was markedly reduced in the central macula (plotted as red horizontal bars in Fig. 6A). In contrast, ZO-1 labeling of the outer plexiform layer and blood vessels was found throughout the retina (acting as an internal positive control). Double labeling against rhodopsin (green in Fig. 6A-F) showed that rods were present more centrally than the OLM (compare red and green horizontal bars in Fig. 6A). High magnification images (Fig. 6D, E) demonstrated this further. Interestingly, the "OLM line" in the OCT (Fig. 1E, 5B) did not match the ZO-1 labeling and, like the IS/OS, correlated better with the area where rods had been depleted (green horizontal bar in Fig. 6A). Near the fovea some residual ZO-1 staining could be detected in the location of the OLM (arrowhead in Fig. 6F). However, this was much weaker than the staining of the OLM in the unaffected periphery.

We also compared the distribution of the OLM markers with Müller cells. To this end we studied an adjacent section (411) with an antibody against occludin (green in Fig. 6G-L), which is also a tight junction protein and an alternative label for the OLM. In addition we used an antibody against RLBP1 (also known as CRALBP, red in Fig. 6G-L) to label Müller cells. The area of Müller cell depletion (green horizontal bars in Fig. 6A) matched the area of macular pigment loss well (yellow arrows in Fig. 6), confirming our findings based on vimentin staining (Fig. 2). Furthermore, the area of Müller cell depletion correlated with the loss of the OLM marker occludin (red horizontal bar in Fig. 6G). On the other hand, as shown for ZO-1 labeling, the occludin staining of the OLM did not have an obvious correlate in the OCT. Furthermore, as with ZO-1, there was very weak punctate staining in the location of the OLM in the fovea (arrowhead in Fig. 6L).

**DISCUSSION**

In this study we have analyzed one postmortem eye from a single MacTel type 2 case. It is not straight forward to extrapolate findings from a single patient towards general disease mechanisms in MacTel type 2. However, this limitation has in this study to some degree been compensated for by the precision of our postmortem analysis and by the matching of clinical data with histology. We demonstrated here that this advanced histology approach of matching clinical data with immunohistochemistry can be useful to learn more about an uncommon disease, such as MacTel type 2, where it is difficult to obtain postmortem material.

We have previously described Müller cell depletion in the macula of a MacTel type 2 case. Here we describe the same finding in a second case, suggesting that Müller cell depletion is a characteristic feature of MacTel type 2. Two cases are not sufficient to make statistically significant statements. Nevertheless, it can be argued that the occurrence of this very unusual phenotype (we are not aware of any other instances where Müller cell loss in the macula has been reported) in the two MacTel type 2 cases so far studied is most likely more than just a coincidence.

It could be argued that Müller cells are not truly lost, but instead downregulate their usual markers and can no longer be detected by immunohistochemistry. However, the fact that in this (and the previous) study three different Müller cell markers (vimentin, GS and RLBP1) disappeared from the macula makes this an unlikely scenario. Also, even if such de-differentiated cells would be formed, they certainly could not be regarded as functional Müller cells. Moreover, both samples (in the previous and the current study) had a tendency to split horizontally during embedding. This suggests a loss of stability across the retinal thickness, which is consistent with a loss of functional Müller cells.

The spatial correlation between macular pigment depletion and functional Müller cell loss demonstrated in our study is a further indication that Müller cell loss is a specific feature of MacTel type 2. Indeed, because of the good correlation it is tempting to speculate that the two features are mechanistically linked. For instance, it is possible that Müller cells are critically involved in the storage of macular pigment or in the metabolism that leads to the accumulation of macular pigment in the retina. Macular pigment depletion could therefore be a direct indication of Müller cell death or dysfunction. However, it is important to note that both MacTel type 2 patients that have been studied by postmortem histology so far, have had advanced disease.

Macular pigment loss occurs early during MacTel type 2 and it is not known yet whether this correlates with Müller cell loss also during the early stages of the disease. Nevertheless, the pronounced loss of Müller cells found in two patients supports the emerging view that MacTel type 2 is not primarily a vascular disease, as its name suggests, but rather a degenerative condition affecting primarily glial cells and neurons.

Because the IS/OS line is widely regarded to originate from the mitochondria rich ellipsoid region in the inner segments of cones and rods, it was surprising to find relatively normal appearing cones with clearly detectable mitochondria in the nasal macula. In the previously described MacTel type 2 case no functional or OCT data was available that could be correlated with photoreceptor histology. In contrast, the patient in this study had a dense, predominantly temporal scotoma and showed characteristic loss of the IS/OS line on OCT in the temporal and nasal macula. Importantly, the cones were histologically present in the nasal macula one year after the IS/OS line was found to be missing in OCT. This discrepancy can therefore not be explained by disease progression. Thus, it appears that the absence of the IS/OS line in MacTel type 2 should not be interpreted as a complete loss of photoreceptors but rather as the presence of conditions that degrade the IS/OS signal from cones. Such conditions may also be linked to reduced visual function as it has been shown in a study using 23 patients that the overall area of the IS/OS break in en face OCT imaging correlates with aggregate retinal sensitivity.[27]

A feature that spatially correlated well with IS/OS loss was rod depletion, but whether there is a causal relationship is not clear. Although cones and rods may both contribute to the IS/OS signal seen on OCT, it may also be the case that rod loss in MacTel type 2 directly abolishes the IS/OS line by an as yet unknown mechanism. For instance, the IS/OS line may depend on well aligned photoreceptors, and when rods are lost, cones may lose their normal alignment. The IS/OS line does not stop in all MacTel type 2 patients as sharply as in our sample and sometimes a more gradual fading may occur. This may relate to gradual rod loss. In our patient the IS/OS was also missing in the fovea, where rods are usually not present. This could suggest the presence of an upstream factor that affects both the IS/OS signal and rod survival. Müller cell loss has to be considered a candidate for such an upstream factor, but the area of Müller cell loss was considerably larger than the area where the IS/OS and rods were lost. Therefore the reason why the IS/OS line seen on OCT is lost in MacTel type 2 is not understood.

A further mismatch between clinical data and histology was the loss of the OLM.  Our analysis clearly demonstrated a spatial link between Müller cell loss and the loss of tight junction proteins in the OLM.  Since Müller cell processes are believed to be a critical component of the OLM this was expected.  However, it was surprising to find in the OCT scan a hyper-reflective line in areas where the histology demonstrated an absence of the OLM.  However, in the case of the OLM and IS/OS loss it is possible to explain the mismatch by disease progression because the OCT features may have spread further into the periphery in the final year before death.

In summary, we present here in a patient with advanced MacTel type 2 two strong spatial correlations between clinical and histological data.  Firstly, we found that macular pigment depletion closely matched the loss of Müller cells.  Secondly, there was also a good match between IS/OS loss and rod depletion.  Because macular pigment depletion usually occurs before the IS/OS is lost in MacTel type 2,[28] we may speculate that Müller cell dysfunction is an early and possibly causative feature of MacTel type 2.

**FIGURE LEGENDS**

**Figure 1.** Clinical data from the donor shows characteristic MacTel type 2 features. In fluorescein angiography (**A, B**) perifoveal blood vessels appear telangiectatic during early (**A**) and leaky during late (**B**) stage imaging. Optical coherence tomography (OCT) and microperimetry of the left eye in 2009 (**C, D**) and 2010 (E, F) shows a break in the inner segment/outer segment junction (IS/OS, arrowheads) and loss of function predominantly in the temporal macula. Color fundus images (**G**) and autofluorescence (**H**) were also recorded.

**Figure 2.** Macular pigment and Müller cells are lost from an oval area in the macula. In the dissected globe (**A**) color photography showed loss of macular pigment in the fovea. An oval area in the macula appears less yellow than the rest of the retina. The contrast enhanced blue channel (**B**) from the color fundus photography (**C**) reveals an oval area that matches the macular pigment depletion in the dissected eye (arrows in **A** and **B**). The oval area in **B** is plotted as a dotted yellow circle in **C**. The position of blood vessel (white dots in **C**) in serial wax sections (horizontal lines and numbers in **C**) is matched onto the color fundus photograph. Anti-vimentin immunohistochemistry (red stain in **D-F**) visualizes Müller cells and their lateral distribution is indicated by horizontal red bars in **D**. White boxes in **D** relate to panels **E** and **F**. Stars in **C** and **F** indicate the same large blood vessel.

**Figures 3 and 4 are online only figures**

**Figure 5.** Inner segment/outer segment junction (IS/OS) loss does not match cone but rod loss. The IS/OS loss in OCT (blue area in **A**) is mapped onto the fundus image. The dotted yellow circle outlines the area of macular pigment loss. A central optical coherence tomography (OCT) scan (**B** and green line in **A**) is compared with a central section (**C** and white line **A**) that has been stained with antibodies against LM-opsin (red stain visualizing cones) and COX2 (green stain visualizing mitochondria) in **C-F**. The IS/OS break (blue arrows) does not match with the distribution of opsin (red horizontal bars in **C**) and COX2 (green horizontal bar in **C**). In contrast, in a second central section stained with antibodies against LM-opsin (red stain visualizing cones) and rhodopsin (green stain visualizing rods) in **G-I** the IS/OS

14

break (blue arrows) correlates well with the distribution of rods (green horizontal bars in **G**).  White boxes in **C** relate to panels **D-F** and **G** to panels **H** and **I**. White arrowheads indicate cone depleted areas.  Stars indicate holes in the outer retina in the fovea.

**Figure 6.**  Outer limiting membrane (OLM) loss does not match rod but Müller cell loss.  Stains on a central section show ZO-1 (in red visualizing the OLM) and rhodopsin (green, visualizing rods) in **A-F**.  The distribution of the OLM (red horizontal bars in **A**) does not match the distribution of rhodopsin (green horizontal bar in **A**).  In an adjacent section (**G-L**), stained to show occludin (in red visualizing the OLM) and RLBP1 (also known as CRALBP, in green visualizing Müller cells), the distribution of the OLM (red horizontal bars in **G**) correlates with the distribution of Müller cells (green horizontal bars in **G**).  IS/OS loss is indicated by blue arrows and macular pigment loss by yellow arrows.  White arrowheads indicate the OLM and stars indicate OLM-unrelated ZO-1 staining in the outer plexiform layer.  Green arrowheads indicate Müller cell bodies.  Boxes in **A** relate to panels **B**, **C** and **F**.  Boxes in **B** and **C** related to panels **D** and **F**.  Boxes in **G** relate to panels **H**, **I** and **L**.  Boxes in **H** and **I** related to panels **J** and **K**.
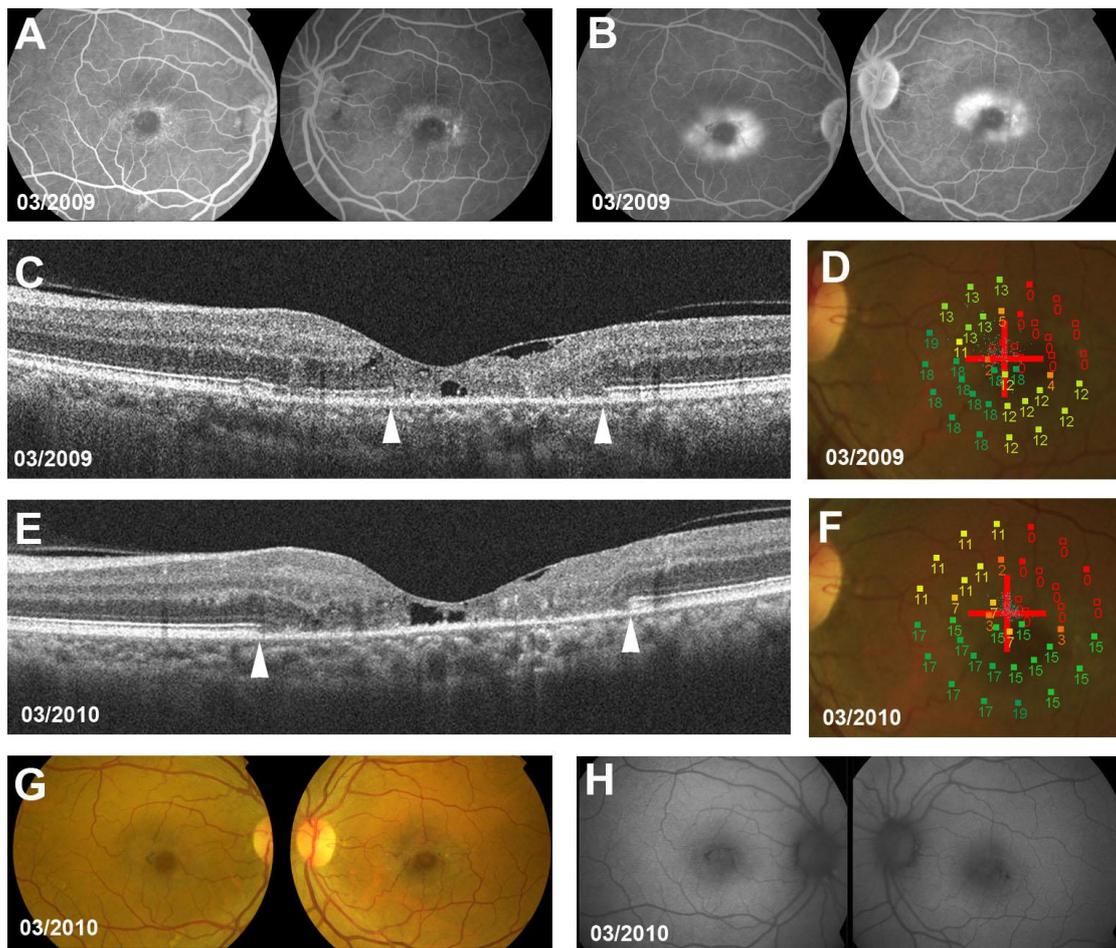
**Figure 1**

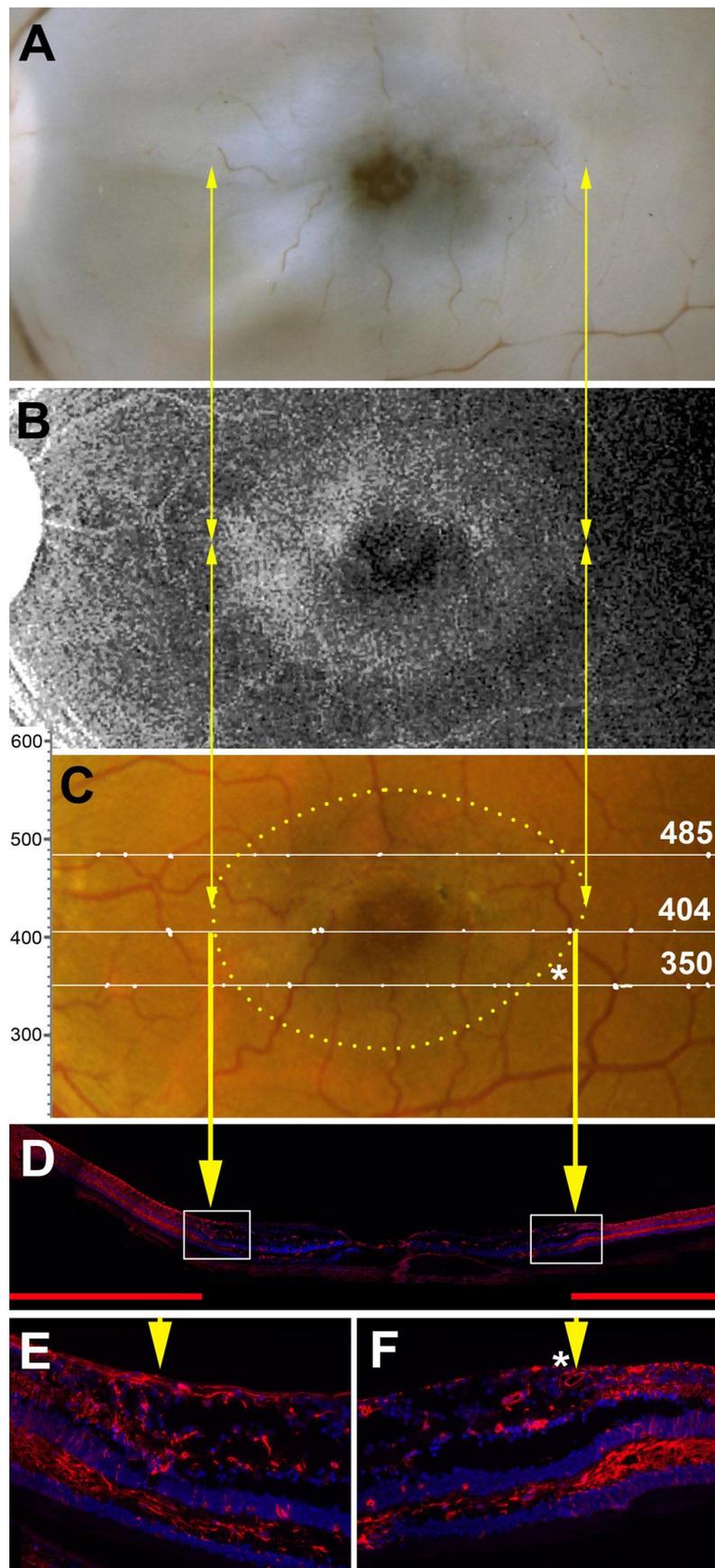A  03/2009

B  03/2009

C  03/2009

D  03/2009

E  03/2010

F  03/2010

G  03/2010

H  03/2010
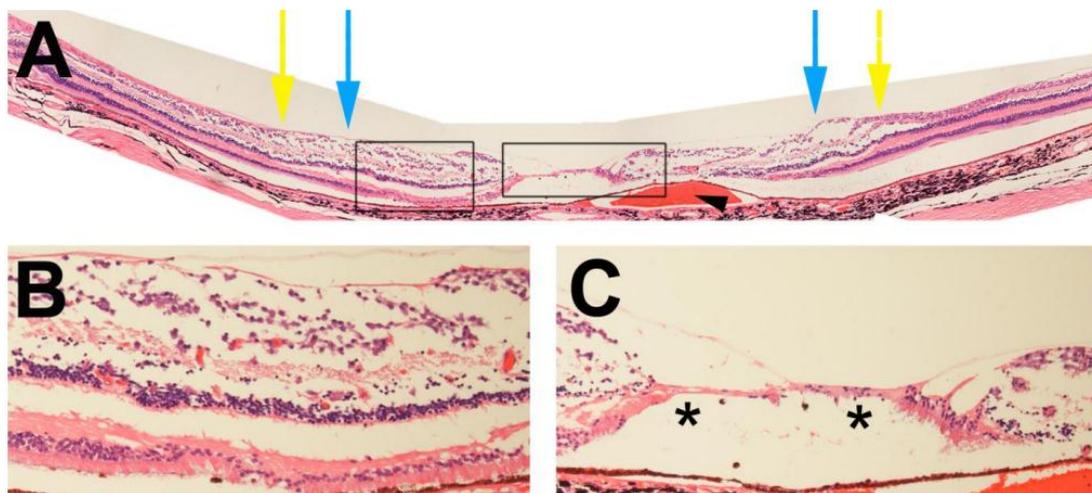
**Figure 2**

**Figure 3 (online only)**



**Figure 3.** Hematoxylin-Eosin staining of a central section illustrates the retinal anatomy in the postmortem sample. Centrally, the processed tissue shows horizontal splits and disintegration (**A**). Nevertheless cell nuclei in the ganglion cell layer and in the inner nuclear layer are present in reasonable numbers (**B**). A large empty space between the retina and the retinal pigment epithelium (RPE) is visible in the fovea (stars in **C**). Blue arrows indicate the boundary of rod loss and yellow arrows indicate the Müller cell loss boundary. The arrowhead indicates a choroidal pool of blood below the RPE, which is most likely a postmortem artifact.
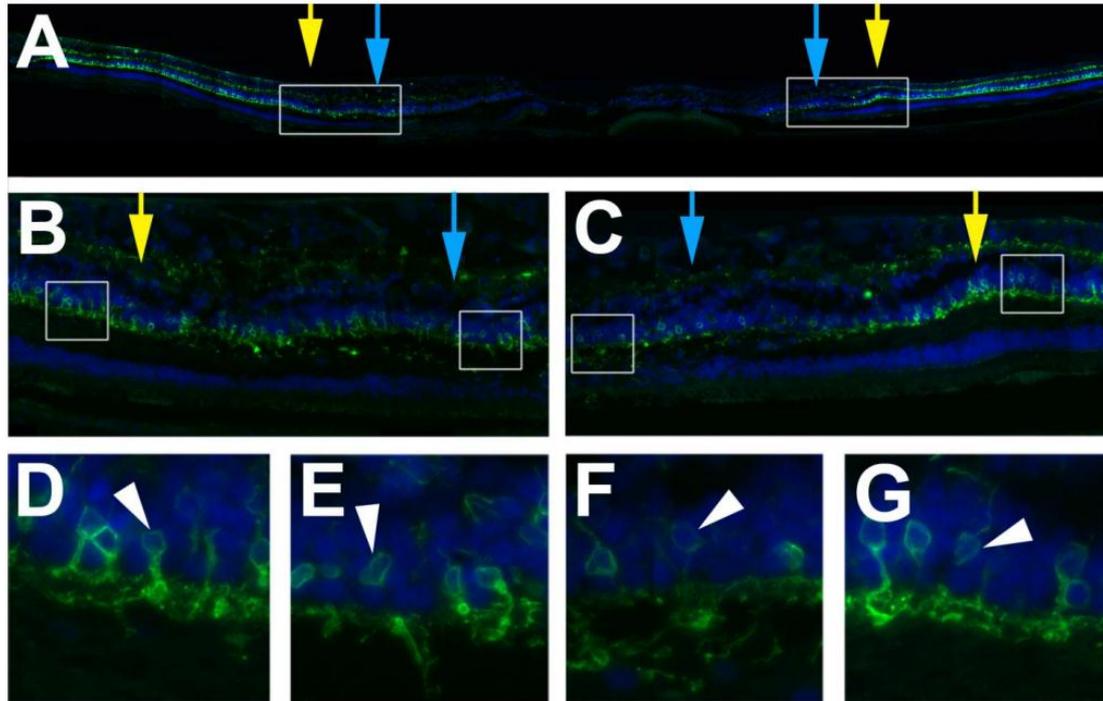
**Figure 4 (online only)**



**Figure 4.** Rod bipolar cells persist in areas of rod loss. Rod bipolar cells were visualized with an antibody against protein kinase C alpha (PRKCA) and found centrally to the boundaries of rod loss (blue arrows) and Müller cell loss (yellow arrows). Arrowheads in **D-G** indicate rod bipolar cell bodies. Boxes in **A** related to panels **B** and **C**. Boxes in **B** relate to panels **D** and **E**. Boxes in **C** relate to panels **F** and **G**.
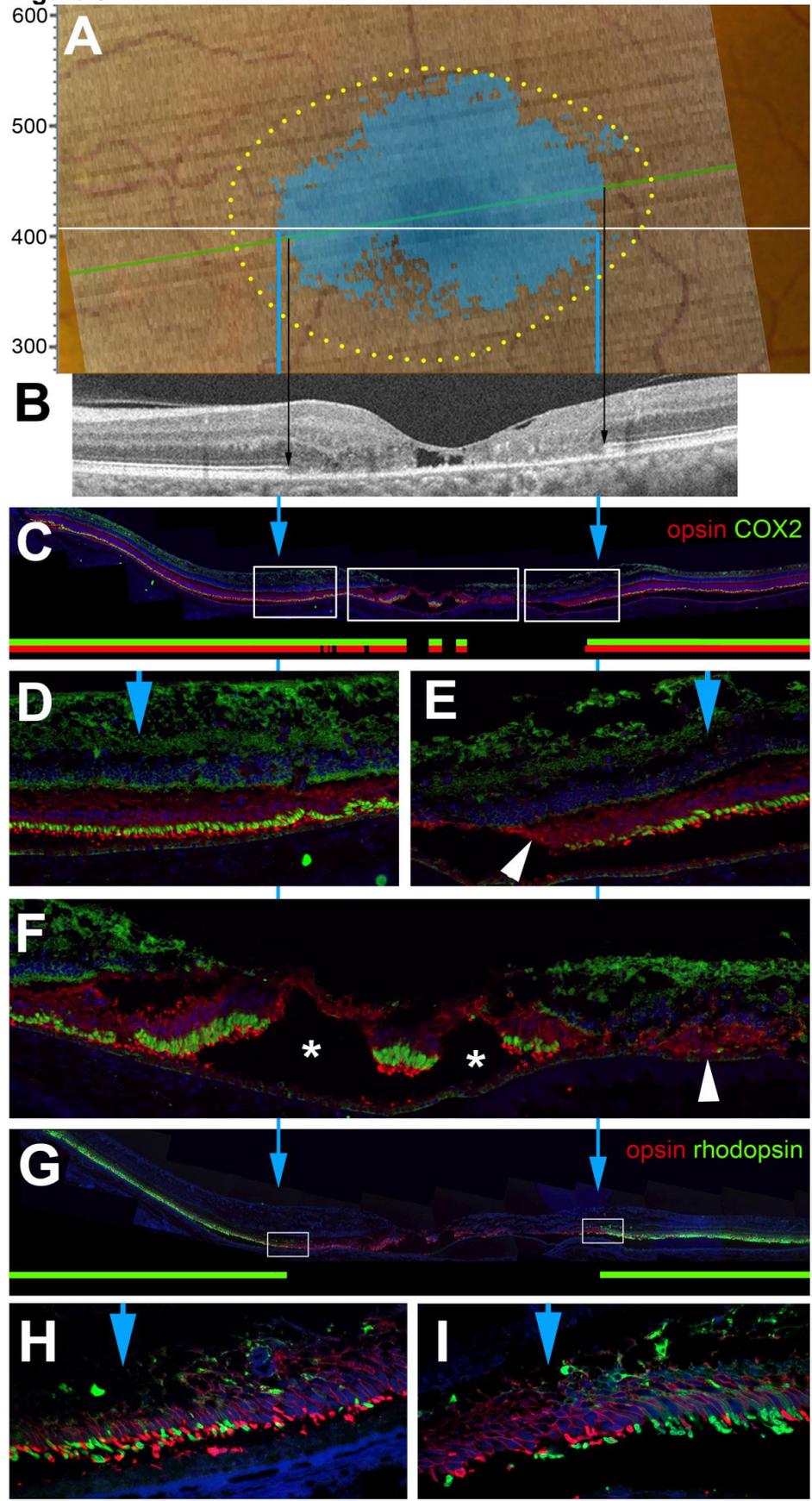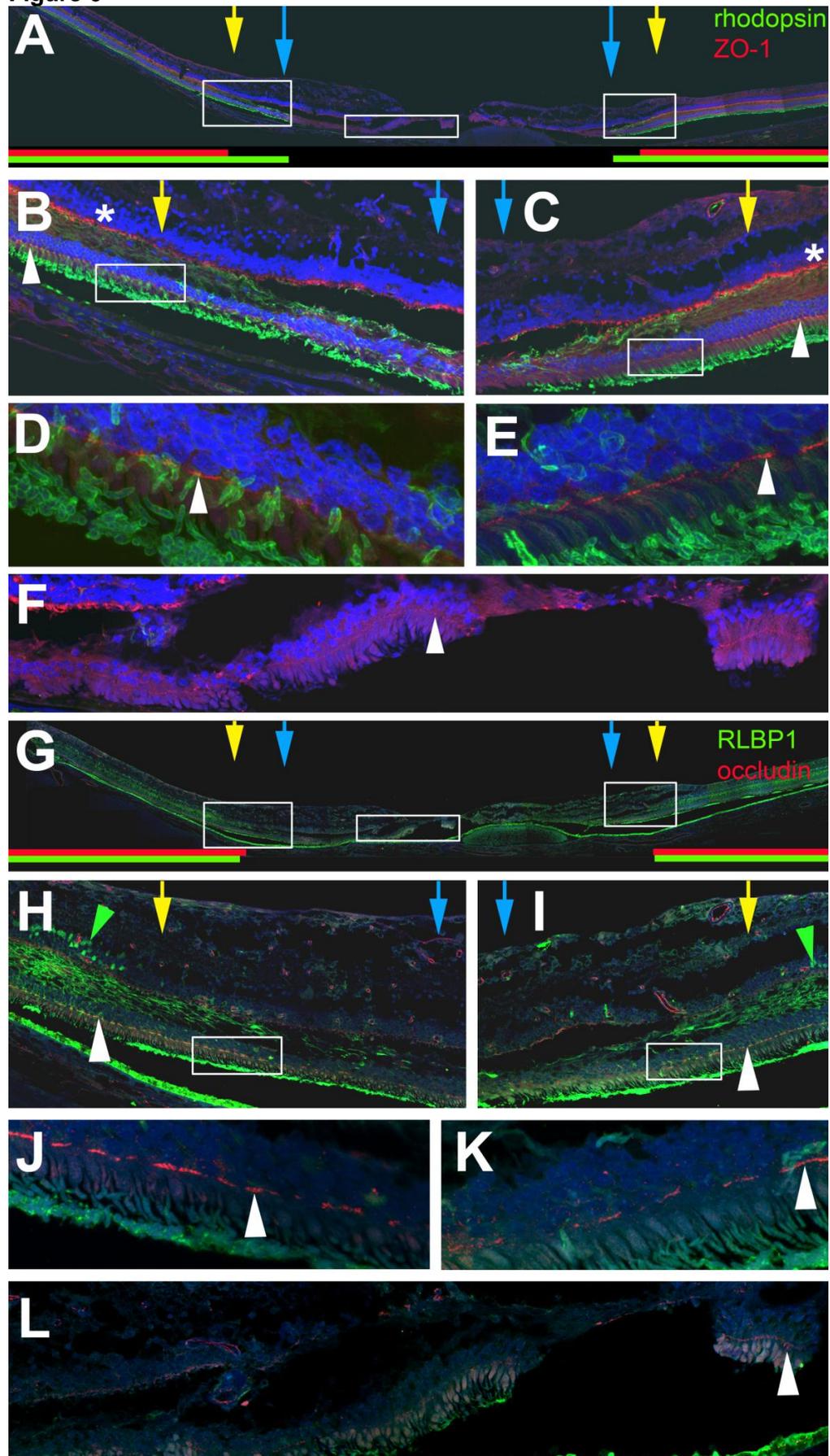
**Figure 5**



opsin COX2

opsin rhodopsin

**Figure 6**

**References**

1. Gass JD, Oyakawa RT. Idiopathic juxtafoveolar retinal telangiectasis. Arch Ophthalmol 1982;100:769-80.

2. Gass JD, Blodi BA. Idiopathic juxtafoveolar retinal telangiectasis. Update of classification and follow-up study. Ophthalmology 1993;100:1536-46.

3. Charbel Issa P, van der Veen RL, Stijfs A, et al. Quantification of reduced macular pigment optical density in the central retina in macular telangiectasia type 2. Exp Eye Res 2009;89:25-31.

4. Helb HM, Charbel Issa P, van der Veen RL, et al. Abnormal macular pigment distribution in type 2 idiopathic macular telangiectasia. Retina 2008;28:808-16.

5. Yannuzzi LA, Bardal AM, Freund KB, et al. Idiopathic macular telangiectasia. Arch Ophthalmol 2006;124:450-60.

6. Gaudric A, Ducos de Lahitte G., Cohen SY, et al. Optical coherence tomography in group 2A idiopathic juxtafoveolar retinal telangiectasis. Arch Ophthalmol 2006;124:1410-9.

7. Maruko I, Iida T, Sekiryu T, Fujiwara T. Early morphological changes and functional abnormalities in group 2A idiopathic juxtafoveolar retinal telangiectasis using spectral domain optical coherence tomography and microperimetry. Br J Ophthalmol 2008;92:1488-91.

8. Krivosic V, Tadayoni R, Massin P, et al. Spectral domain optical coherence tomography in type 2 idiopathic perifoveal telangiectasia. Ophthalmic Surg Lasers Imaging 2009;40:379-84.

9. Clemons TE, Gillies MC, Chew EY, et al, MacTel Research Group. The National Eye Institute Visual Function Questionnaire in the Macular Telangiectasia (MacTel) Project. Invest Ophthalmol Vis Sci 2008;49:4340-6.

10. Finger RP, Charbel Issa P, Fimmers R, et al. Reading performance is reduced by parafoveal scotomas in patients with macular telangiectasia type 2. Invest Ophthalmol Vis Sci 2009;50:1366-70.

11. Charbel Issa P, Helb HM, Rohrschneider K, et al. Microperimetric assessment of patients with type 2 idiopathic macular telangiectasia. Invest Ophthalmol Vis Sci 2007;48:3788-95.

12. Charbel Issa P, Foerl M, Helb HM, et al. Multimodal fundus imaging in foveal hypoplasia: combined scanning laser ophthalmoscope imaging and spectral-domain optical coherence tomography. Arch Ophthalmol 2008;126:1463-5.

13. Schmitz-Valckenberg S, Fan K, Nugent A, et al. Correlation of functional impairment and morphological alterations in patients with group 2A idiopathic juxtafoveal retinal telangiectasia. Arch Ophthalmol 2008;126:330-5.

14. Powner MB, Gillies MC, Tretiach M, et al. Perifoveal Muller cell depletion in a case of macular telangiectasia type 2. Ophthalmology 2010;117:2407-16.

15. Chew EY, Murphy RP, Newsome DA, Fine SL. Parafoveal telangiectasis and diabetic retinopathy. Arch Ophthalmol 1986;104:71-5.

16. Clemons TE, Gillies MC, Chew EY, et al, MacTel Research Group. Baseline characteristics of participants in the Natural History Study of Macular Telangiectasia (MacTel) MacTel Project Report No. 2. Ophthalmic Epidemiol 2010;17:66-73.

17. Casswell AG, Chaine G, Rush P, Bird AC. Paramacular telangiectasis. Trans Ophthalmol Soc U K 1986;105:683-92.

18. Millay RH, Klein ML, Handelman IL, Watzke RC. Abnormal glucose metabolism and parafoveal telangiectasia. Am J Ophthalmol 1986;102:363-70.

19. Charbel Issa P, Berendschot TT, Staurenghi G, et al. Confocal blue reflectance imaging in type 2 idiopathic macular telangiectasia. Invest Ophthalmol Vis Sci 2008;49:1172-7.

20. Kolb H, Zhang L, Dekorver L. Differential staining of neurons in the human retina with antibodies to protein kinase C isozymes. Vis Neurosci 1993;10:341-51.

21. Kolb H, Zhang L. Immunostaining with antibodies against protein kinase C isoforms in the fovea of the monkey retina. Microsc Res Tech 1997;36:57-75.

22. Charbel Issa P, Troeger E, Finger R, et al. Structure-function correlation of the human central retina. PLoS One [serial online] 2010;5:e12864. Available at: http://www.plosone.org/article/info%3Adoi%2F10.1371%2Fjournal.pone.0012864.

23. Fernandez EJ, Hermann B, Povazay B, et al. Ultrahigh resolution optical coherence tomography and pancorrection for cellular imaging of the living human retina. Opt Express [serial online] 2008;16:11083-94. Available at: http://www.opticsinfobase.org/oe/abstract.cfm?uri=oe-16-15-11083.

24. Hood DC, Zhang X, Ramachandran R, et al. The inner segment/outer segment border seen on optical coherence tomography is less intense in

patients with diminished cone function. Invest Ophthalmol Vis Sci 2011;52:9703-9.

25. Spaide RF, Curcio CA. Anatomical correlates to the bands seen in the outer retina by optical coherence tomography: literature review and model. Retina 2011;31:1609-19.

26. Hoang QV, Linsenmeier RA, Chung CK, Curcio CA. Photoreceptor inner segments in monkey and human retina: mitochondrial density, optics, and regional variation. Vis Neurosci 2002;19:395-407.

27. Sallo FB, Peto T, Egan C, et al, MacTel Study Group. The IS/OS junction layer in the natural history of type 2 idiopathic macular telangiectasia. Invest Ophthalmol Vis Sci 2012;53:7889-95.

28. Gillies MC, Zhu M, Chew E, et al. Familial asymptomatic macular telangiectasia type 2. Ophthalmology 2009;116:2422-9.